

# A Novel Beamforming Scheme for Mobile-to-Mobile Millimeter Wave Communications

Yi Tan<sup>1</sup>, Cheng-Xiang Wang<sup>1</sup>, Qiuming Zhu<sup>2</sup>, Zhi Zhang<sup>3</sup>, Zhonghua Wang<sup>4</sup>, Jie Huang<sup>5</sup>, and Rui Feng<sup>5</sup>

<sup>1</sup>Institute of Sensors, Signals and Systems, School of Engineering & Physical Sciences, Heriot-Watt University, Edinburgh EH14 4AS, UK.

<sup>2</sup>College of Electronic and Information Engineering, Nanjing University of Aeronautics and Astronautics, Nanjing 211106, Jiangsu, China.

<sup>3</sup>Information Engineering College, Zhijiang College of Zhejiang university of Technology, Hangzhou 312030, Zhejiang, China.

<sup>4</sup>Business Area Networks, Ericsson Stockholm, Isafjordsgatan 14E, 16480 Stockholm, Sweden.

<sup>5</sup>Shandong Provincial Key Lab of Wireless Communication Technologies, Shandong University, Jinan 250100, Shandong, China.

Email: yi.tan@hw.ac.uk, cheng-xiang.wang@hw.ac.uk, zhuqiuming@nuaa.edu.cn, zhangzhi@zjc.zjut.edu.cn,

zhonghua.wang@ericsson.com, hj\_1204@sina.cn, fengxiurui604@163.com

**Abstract**—Due to using beamforming technology in millimeter wave (mmWave) communication, the movement of transmitter (Tx) and receiver (Rx) will cause the mis-alignment of Tx and Rx beams. In order to deal with this problem, a novel physical layer beamforming scheme is proposed in this paper, namely, double Gaussian beams (DGBs) scheme, which treats the static and moving Tx/Rx scenarios in the same manner. We model the DGBs channels by three Markov states, and the connection ratio of Markov state is used as the metric to study the performance of DGBs scheme from the channel point of view. We show that the DGBs channels have very similar light-of-sight (LOS) state connection ratio compared with that of the measured mmWave channels based on similar set up of the Tx and Rx beams.

**Index Terms**—mmWave channel, beam alignment, double Gaussian Beams, Markov states, connection ratio.

## I. INTRODUCTION

Beamforming technique is widely used in mmWave communication systems [1], and it is typical that both the Tx and Rx are casting beams to align with each other for transmitting information. If the Tx or Rx moves, the beams will be mis-aligned and the communication between Tx and Rx could be broken if there is no robust solution to re-align the beams. The studies about the impact of user mobility on mmWave communications can be found in [2].

A robust beam alignment scheme is required in mmWave communications. The related state-of-the-art researches are mainly as follows: adaptive beamforming [3], [4], hybrid antenna array [5], two layers of beam alignment [6], [7], beam switching [8], dual connectivity [9], beam training [10], intelligent beam search and tracking algorithms [11], etc.

Those above mentioned schemes require the system level controls from protocol and application layers. They are relatively complicated to be implemented in the mobile to mobile (M2M) mmWave communication scenarios. In this paper, we propose a simple physical layer DGBs scheme for M2M mmWave communications. It treats both the static and moving Tx and Rx scenarios in the same manner.

The rest of this paper is organized as follows. Section II introduces the DGBs scheme. In Section III, we model both the DGBs channels and measured mmWave channels by

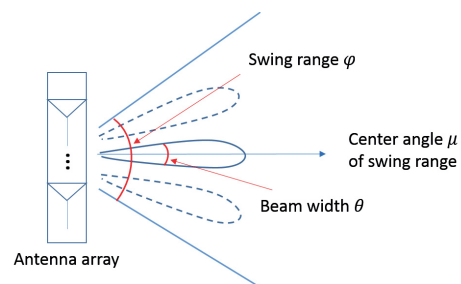


Fig. 1. Construction of one Gaussian beam based on beamforming technology.

three Markov states. In Section IV, the connection ratios of three Markov states DGBs channels are estimated, and the connection ratios between the DGBs channels and measured mmWave channels are compared. Conclusions are finally drawn in Section V.

## II. DOUBLE GAUSSIAN BEAMS COMMUNICATION

In optical and visible light communication (VLC) [12]–[14], Tx transmits a Gaussian beam with a radiation pattern that gradually spreads as it propagates to further distance. The feature of Gaussian beam is that, the transverse power density is Gaussian distributed. Analogously, we can create a similar Gaussian beam with beamforming technology and use it to overcome the mis-alignment of Tx and Rx beams caused by the movement in mmWave communications.

### A. Gaussian Beam

Assume there is a radio system equipped with antenna arrays as in Fig. 1, and it uses beamforming technology during signal transmission/receipt. We define a flashing rate  $\gamma$  as how many beams can be generated per second. All the generated beams have fixed beamwidth  $\theta$ , and the pointing angles of them are limited within a swing range  $\psi$  ( $\theta \ll \psi$ ). We assume  $\mu$  is the center angle of swing range and  $\sigma$  is the angular variation of the center of beam. Statistically, the transverse power density in the swing range is Gaussian distributed  $N(\mu, \sigma)$  along the propagation direction. Based

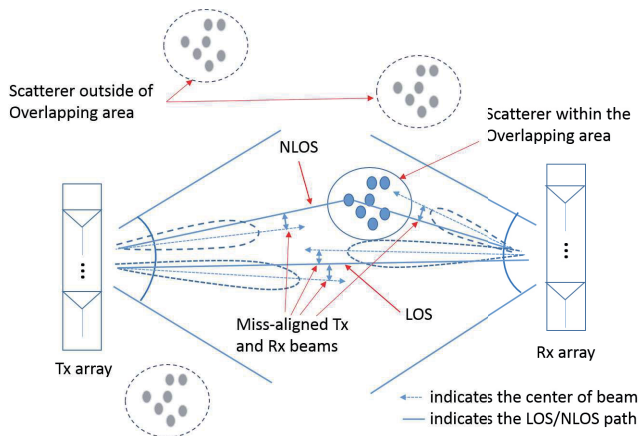


Fig. 2. DGBs channels.

on [15], approximately 99.7 percent power lies within three standard deviations ( $\mu \pm 3\sigma$ ) of the swing range, therefore, we define the relationship of  $\psi$  and  $\sigma$  as

$$\frac{\psi}{2} \approx +3\sigma \approx -3\sigma. \quad (1)$$

### B. DGBs Communication Scheme

We apply the Gaussian beams to both Tx and Rx in channel scenario as in Fig. 2. If we consider the instantaneous alignment of Tx and Rx beams as one connection, then, the communications between Tx and Rx are keeping connected and disconnected as long as there is an overlapping area of the Tx and Rx Gaussian beams. We define a connecting ratio  $p$  as a metric to study the successful connections between the Tx and Rx.

$$p = \frac{\text{Successful connections per second}}{\gamma}. \quad (2)$$

The proposed communication scheme could be used for data package transmissions as the etheral net does. Each data package is not guaranteed to be delivered to the receiver, but the Tx is trying the best to deliver them.

We can use high-speed radio frequency (RF) switch in the implement of Gaussian beam in reality. The speed of beam switching could be as short as a few nanoseconds [16], and the RF switches with such switching speed are widely used in the industry. In the rest of paper, we assume that both Tx and Rx can generate 20 random beams per millisecond, i.e.,  $\gamma = 20,000$ .

## III. MARKOV STATES MMWAVE CHANNELS

For the typical mmWave communications with beamforming technology, the directional wireless channels between Tx and Rx can be modeled by three Markov states. If the Tx and Rx beams are aligned with each other during communication, the channels can be considered in LOS state. When Tx/Rx moves or rotates, the beams become mis-aligned. If the communication could be maintained based on strong non-light-of-sight (NLOS) signals, the channels can be considered

in NLOS state. Otherwise, it is in Outrage state. For the Rx side, the received directional channel impulse responses (D-CIRs)  $h(\tau)$  can be modeled as

$$h(\tau) = \begin{cases} h^{\text{LOS}}(\tau), & p_{\text{LOS}} \\ h^{\text{NLOS}}(\tau), & p_{\text{NLOS}} \\ \text{Null}, & 1 - p_{\text{LOS}} - p_{\text{NLOS}} \end{cases} \quad (3)$$

where  $p_{[*]}$  is the percentage of D-CIRs in LOS state or NLOS state over the flash rate  $\gamma$ .

### A. Three Markov States DGBs Channels

Assume that there is an object within the DGBs channel as in Fig. 2. The center of this object is randomly located, and it is large enough to block the LOS path between Tx and Rx. In every instantaneous time, the Rx received D-CIR  $h(\tau)$  falls into one of three Markov states. When the Tx and Rx beams are cast to each other directly within a tolerable mis-aligned angle, the DGBs channel is in LOS state. When the Tx and Rx all cast beams to the object within a tolerable mis-aligned angle and the scattered signals could maintain the communication between them, the DGBs channel is in NLOS state. In the cases that the object blocks the LOS path between the Tx and Rx and the angles of Tx and Rx beams outwith the tolerable mis-aligned angles, the DGBs channel is in the Outrage state.

The one-step transition probabilities of Markov states are highly environmental dependent within the overlapping area. Due to plenty of work remains to implement it in hardware, we are not able to perform the real measurement of DGBs channels at the moment (the channel measurement in the following sub-section is not based on DGB scheme). Therefore we leave it for future study. However, compared with the high flashing rate of DGBs, we assume that the DGBs channel is stationary for a certain limited of time while the Tx and Rx move in relatively slow speed. We consider the limiting distribution of Markov states [15] in this case is related to  $p_{\text{LOS}}$ ,  $p_{\text{NLOS}}$ , and  $1 - p_{\text{LOS}} - p_{\text{NLOS}}$ . The limiting distribution of Markov states is the key parameters to achieve the conclusion.

### B. Channel Measurement and Three Markov States Measured Channels

The directional antennas were widely used in the mmWave channel measurements in the literature [17]–[19]. In this section, we choose one relatively simple and typical mmWave channel measurement as an example, and illustrate that the measured directional mmWave channels can also be modeled by three Markov states.

1) *Channel Measurement*: The indoor mmWave channel measurement [20] was conducted in Shandong University, China, a static office environment as in Fig. 3. It was performed by Keysight N5227A vector network analyzer (VNA), and the frequency range was from 59 to 61 GHz. The standard horn antennas with 25 dBi gain and 3-dB beamwidth of  $10^\circ$  at 60 GHz were used in both Tx and Rx, which were both at 1.6 m height. The Tx antenna was placed on the antenna positioner at Tx1, and rotated from  $0^\circ$  to  $355^\circ$  in azimuth

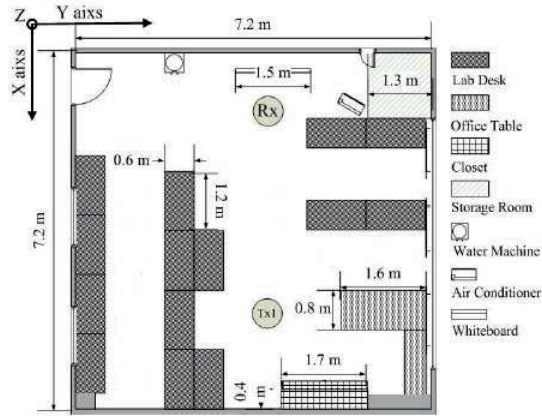


Fig. 3. Layout of an indoor office environment in Shandong University [20].

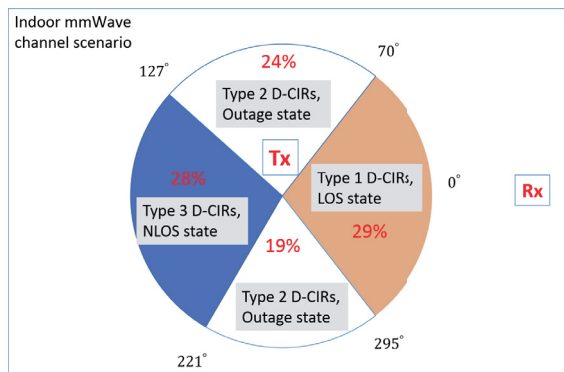


Fig. 4. Angular separated three typical D-CIRs in three Markov states (Tx rotates and Rx hold still).

angles with step of  $5^\circ$ , while the horn antenna at Rx was held still pointing to Tx.

2) *Three Markov States Measured Channels*: In the data analysis, based on the estimated angular stationarity regions (ASRs) of the channel, root mean square (RMS) delay spreads (DSs), and K-factors, three types of measured D-CIRs have been found [20]. In this paper, we consider those three typical D-CIRs as three Markov states. We define the D-CIRs contain one strong LOS component and a few weak NLOS components are in the LOS state; those contain one relatively strong NLOS component and a few weak NLOS components are in the NLOS state; and those contain only weak NLOS components are in the Outage state.

Based on the three separated typical D-CIRs in azimuth angles in [20]

- Type 1: D-CIRs measured at the azimuth angles smaller than  $70^\circ$  and larger than  $295^\circ$
- Type 2: D-CIRs measured at the azimuth angles between  $70^\circ$  and  $125^\circ$  & between  $215^\circ$  and  $295^\circ$
- Type 3: D-CIRs measured at the azimuth angles between  $125^\circ$  and  $215^\circ$

Fig. 4 shows both the locations and percentage of angular coverage areas of those three typical D-CIRs in each Markov

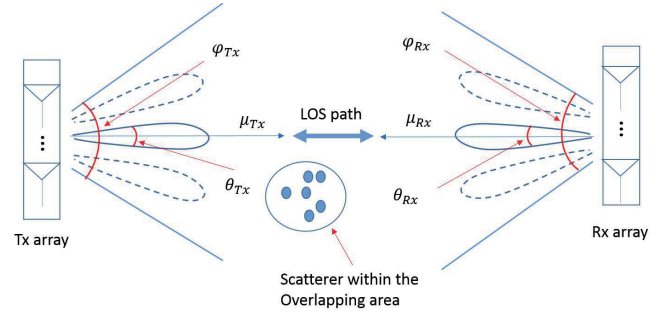


Fig. 5. DGBs channels in the located case.

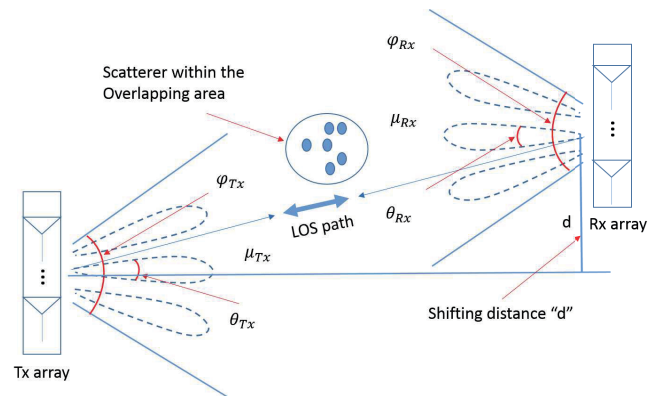


Fig. 6. DGBs channels in the dislocated case (shifting distance is  $d$ ).

state. They are: 29% in LOS state, 28% in NLOS state, and 43% in Outage state.

#### IV. STUDY AND COMPARISON OF CONNECTION RATIOS

The static and moving Tx/Rx scenarios are treated in the same manner in DGBs scheme. For less confusing, we consider the Tx and Rx that are facing each other precisely in Fig. 5 as located case, and consider the Tx and Rx that are not facing each other precisely with a shifting distance in Fig. 6 as dislocated case. We assume those located and dislocate cases are independent of the movements of Tx and Rx.

The studies of DGBs channels are based on simulations in this paper. However, we compare the connection ratios of DGBs channels with those estimated from the real mmWave channel measurement described previously.

##### A. Connection Ratios of Markov States DGBs Channels

1) *Synchronized DGBs Channels*: We assume that the Tx and Rx are casting  $\gamma$  beams per second to each other, and the timings of casting each simultaneous beam at both Tx and Rx sides are synchronized. In the simulation, we let the distance between the Tx and Rx is 10 m; the swing ranges of Tx and Rx Gaussian beams,  $\psi_{Tx}$  and  $\psi_{Rx}$ , are both  $60^\circ$ ; the variation of center of Gaussian beam  $\sigma$  is  $10^\circ$  at both the Tx and Rx side; and the shifting distance  $d$  is 2 m for the dislocated case. We also assume that the object is slim, its width could be ignored and its length is 1 m (about 8.7% size of DGBs channel area in

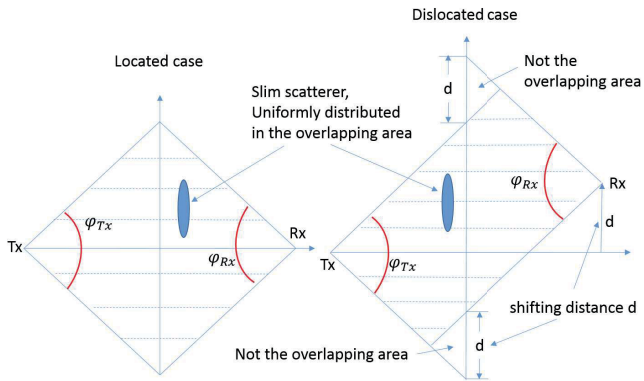


Fig. 7. The DGBs overlapping area for both the located and dislocated cases.

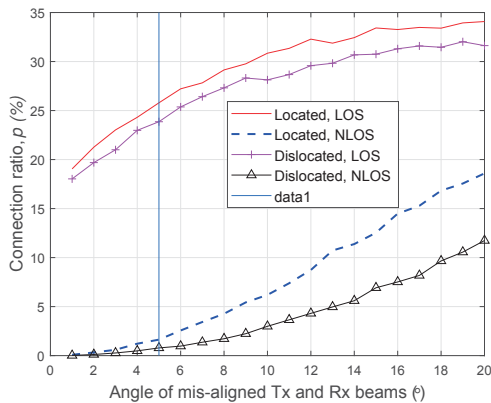


Fig. 8. Synchronized DGBs channels (swing ranges  $\psi_{Tx} = \psi_{Rx} = 60^\circ$ , length of vertical positioned slim object is 1 m, distance between Tx and Rx is 10 m, and the shifting distance  $d$  is 2 m for the dislocated case).

y axis), which is long enough to block the LOS path between Tx and Rx. We position it vertically in the DGBs overlapping area as in Fig. 7 following the uniform distribution.

Note that we do not consider the beamwidths of Tx and Rx beams,  $\theta_{Tx}$  and  $\theta_{Rx}$ , in the simulation. Instead, we assume that the beamwidths are always suitable to obtain the simulation results (always be two times of each angle of mis-aligned beams for example). We do not consider the frequencies of mmWave signals in the simulations neither. We let the distance between Tx and Rx is 10 m simply due to the high attenuation of mmWave signals.

Fig. 8 shows the connection ratios of DGBs channels in LOS and NLOS Markov states vs. the angles of mis-aligned Tx and Rx beams from  $1^\circ$  to  $20^\circ$ . We can see that for both the located and dislocated cases, as we increase the angle of mis-aligned Tx and Rx beams, the connection ratios of both LOS and NLOS states become higher. The connection ratios of LOS states in the located case are from 18.92% to 33.79%, and are from 17.93% to 31.74% in the dislocated case with the shifting distance  $d = 2$  m. The connection ratios of NLOS states in the located case are from 0.025% to 18.83%, and are from 0.025% to 11.7% in the dislocated case.

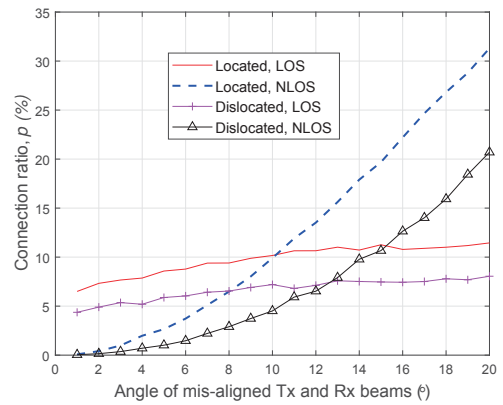


Fig. 9. Synchronized DGBs channels (swing ranges  $\psi_{Tx} = \psi_{Rx} = 60^\circ$ , length of vertical positioned slim object is 3 m, distance between Tx and Rx is 10 m, and the shifting distance  $d$  is 2 m for the dislocated case).

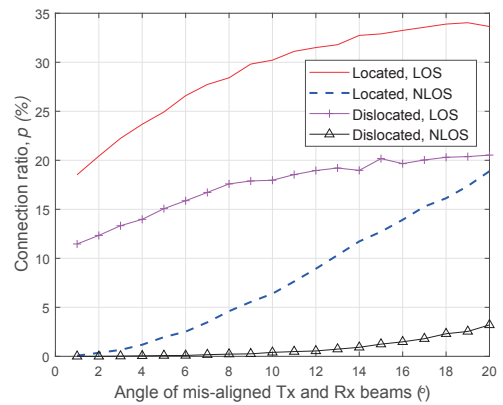


Fig. 10. Synchronized DGBs channels (swing ranges  $\psi_{Tx} = \psi_{Rx} = 60^\circ$ , length of vertical positioned slim object is 1 m, distance between Tx and Rx is 10 m, and the shifting distance  $d$  is 4 m for the dislocated case).

In Fig. 9, we increase the length of vertical positioned slim object to 3 m, and keep other settings as in Fig. 8. We can observe that for both the located and dislocated cases, the LOS state connection ratios are decreased while the NLOS state connection ratios are increased. It makes sense that as the length of slim objects increases, the chance that the LOS paths between the Tx and Rx are blocked increases, while the chance that the communication between Tx and Rx could be maintained based on the signals that are scattered by the slim object increases.

In Fig. 10, we let the shifting distance  $d$  be 4 m, and keep other settings the same as in Fig. 8. We can observe that the connection ratios of both LOS and NLOS states in the dislocated case decrease compared with those in Fig. 8. The reason is that when the shifting distance  $d$  increases, the size of DGBs overlapping area decreases, so as the connection ratios of DGBs channels in both LOS and NLOS states. We have found similar phenomena in the simulations with different swing ranges ( $120^\circ$  and  $60^\circ$ ), different distances between the

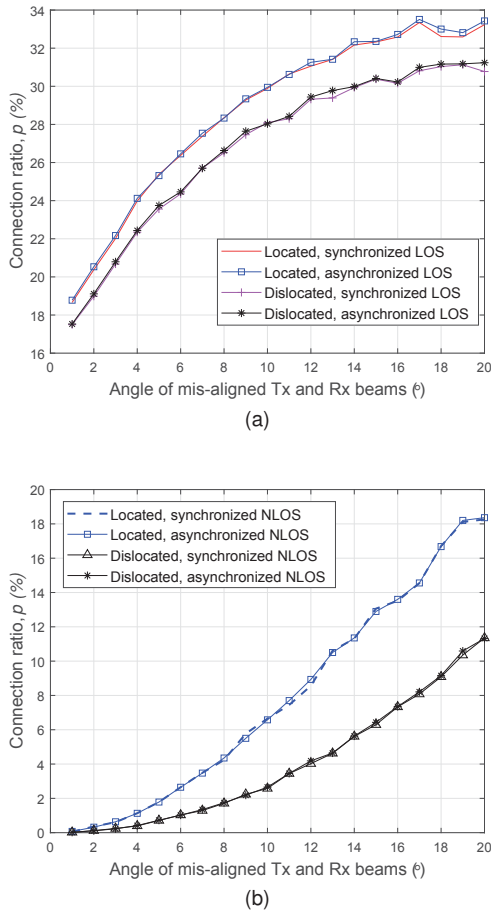


Fig. 11. Both synchronized and asynchronous DGBs channels (swing range  $\psi_{Tx} = \psi_{Rx} = 60^\circ$ , length of vertical positioned slim object is 1m, distance between Tx and Rx is 10 m, and the shifting distance  $d$  is 2 m for the dislocated case): (a) LOS states, and (b) NLOS states.

Tx and Rx, and different lengths of the slim object. As the DGBs overlapping area decreases, the connection ratios of DGBs channels decrease accordingly.

2) *Asynchronous DGBs Channels*: We assume that the Tx and Rx lost the synchronization of timing to cast each simultaneous beam. We let the Tx casts each simultaneous beam earlier than Rx does (vice versa) with the time difference of 50% beam duration. We count the overall duration of connections in LOS or NLOS state over one second as connection ratio. From the results in Fig. 11, we can see that the synchronized and asynchronous connection ratios of LOS and NLOS states in both located and dislocated cases are almost the same. If we change the time difference to other values, the connection ratios in asynchronous DGBs channels are also very close to those in synchronized DGBs channels. This indicates that the synchronization of instantaneous Tx and Rx beams has no significant impact on the connection ratios of DGBs channels.

### B. Connection Ratios of Markov States Measured mmWave Channels

In Section III-B, we have estimated the percentage of angular coverage areas of three typical D-CIRs in each Markov state based on [20]. If we consider the channel measurement as an unchanged environment, and the base station is kept casting one stable beam to the users without changing the beam angle. Then, we can assume that if one person is randomly walking in such a channel environment, she/he can connect to the base station when she/he is walking inside of the angular coverage areas of LOS and NLOS states. In this case, the percentages of angular coverage areas of Markov states can be considered as the limiting distribution of Markov states, which are also the connection ratios of directional mmWave channels in those Markov states. They are: 29% for the connection ratio of LOS state, 28% for the connection ratio of NLOS state, and 43% for the connection ratio of Outage state.

### C. Comparison of Connection Ratios

Assume the beamwidths of Tx and Rx beams,  $\theta_{Tx}$  and  $\theta_{Rx}$ , used in DGBs communications are  $10^\circ$ , which are the same as those of the horn antennas used in the aforementioned channel measurement. In order to keep the connection between Tx and Rx in “good situation”, we let the aligned Tx and Rx beams are at least 50% overlapped in term of beamwidth. Therefore, the mis-aligned angle of Tx and Rx beams should be limited to  $5^\circ$ , and we can find the corresponding connection ratios from Fig. 8. In the located case, the connection ratio of LOS state is 25.48%, and the connection ratio of NLOS state is 1.66%. In the dislocated case, the connection ratio of LOS state is 23.65%, and the connection ratio of NLOS state is 0.84%.

Compared with the LOS state connection ratios estimated from the channel measurement, the LOS state connection ratio of DGBs channels in the located case is 3.52% lower, and in the dislocated case, it is 5.35% lower. However, the NLOS state connection ratios of DGBs channels in both the located and dislocated cases are much lower compared with those estimated from the channel measurement. Because the NLOS state connection ratios are highly environment dependent, and the simulation assumption of DGBs channel is quite different from that in the measured channel (the objects, such as walls, ceiling, windows, and doors, etc., are all scatterers). According to the analysis in Section IV-A1, if we can keep the overlapping area of DGBs channel as large as possible, the acceptable connection ratios as in Fig. 8 can be achieved in M2M mmWave communication under DGBs scheme.

## V. CONCLUSIONS

We have proposed a simple DGBs scheme based on beam-forming technology for M2M mmWave communications in this paper. The Markov states have been utilized to model the DGBs channels, and to model the measured directional mmWave channels in an office environment for comparison purpose. The connection ratio of Markov state has been considered as the metric to study the performance of DGBs scheme from the channel point of view. It has shown that

the DGBs channels have very similar LOS state connection ratios compared with those of the measured mmWave channels based on using the beams with  $10^\circ$  beamwidth. But the NLOS state connection ratios of DGBs channels are much lower, which is related to the environmental differences between the simulation assumption of DGBs channels and the measured mmWave channel. We have found that when the Tx and Rx are in the dislocated case, the connection ratios of both LOS and NLOS states decrease as the size of DGBs overlapping area decreases. We have also found that the synchronization of Tx and Rx beams has no significant impact on the connection ratios of DGBs channels.

Since DGBs scheme a physical layer beam alignment technique, we expect that it requires less system level controls from the protocol and application layers. It is suitable for the communication scenarios that the Tx and Rx are moving all the time. It is also suitable for the mmWave communications at initiation stage, when the Tx and Rx have no knowledge of system configuration on the other side.

#### ACKNOWLEDGMENT

The authors would like to gratefully acknowledge the support of this work from the EU H2020 ITN 5G Wireless project (No. 641985), the EU H2020 RISE TESTBED project (No. 734325), the EU FP7 QUICK project (No. PIRSES-GA-2013-612652), and the EPSRC TOUCAN project (No. EP/L020009/1).

#### REFERENCES

- [1] W. Roh, J. Y. Seol, J. Park, B. Lee, J. Lee, Y. Kim, J. Cho, K. Cheun, and F. Aryanfar, "Millimeter-wave beamforming as an enabling technology for 5G cellular communications: theoretical feasibility and prototype results," *IEEE Commun. Mag.*, vol. 52, no. 2, pp. 106–113, Feb. 2014.
- [2] A. Maltsev, I. Bolotin, A. Lomayev, A. Pudneyev, and M. Danchenko, "User mobility impact on millimeter-wave system performance," in *Proc. EuCAP'16*, Davos, Switzerland, Apr. 2016, pp. 1–5.
- [3] A. Alkhateeb, O. Ayach, G. Leus, and R. Heath, "Channel estimation and hybrid precoding for millimeter wave cellular systems," *IEEE Trans. Signal Process.*, vol. 8, no. 5, pp. 831–846, Oct. 2014.
- [4] H. Huang, K. Liu, R. Wen, Y. Wang, and G. J. Wang, "Joint channel estimation and beamforming design for wide band millimeter wave cellular system," in *Proc. IEEE Globecom 2015 Workshop*, San Diego, USA, Dec. 2015, pp. 1–6.
- [5] J. A. Zhang, X. Huang, V. Dyadyuk, and Y. J. Guo, "Massive hybrid antenna array for millimeter-wave cellular communications," *IEEE Wireless Commun. Mag.*, vol. 22, no. 1, pp. 79–87, Feb. 2015.
- [6] Y. Wang, Z. Shi, Kun Zeng and Peiying Zhu, "Two layers of beam alignment for millimeter-wave communications," in *Proc. DIPDMWC'16*, Moscow, Russia, Jul. 2016, pp. 262–267.
- [7] T. Nitsche, C. Cordeiro, A. B. Flores, E. W. Knightly, E. Perahia, and J. C. Widmer, "IEEE 802.11ad: Directional 60 GHz communication for multi-gigabit-per-second Wi-Fi," *IEEE Commun. Mag.*, pp. 132–141, Dec. 2014.
- [8] V. Va, T. Shimizu, G. Bansal, and R. W. Heath, "Beam design for beam switching based millimeter wave vehicle-to-infrastructure communications," in *Proc. IEEE ICC'16*, Kuala Lumpur, Malaysia, May 2016, pp. 1–6.
- [9] M. Polese, M. Giordani, M. Mezzavilla, S. Rangan, and M. Zorzi, "Improved handover through dual connectivity in 5G mmWave mobile networks," *IEEE J. Sel. Areas Commun.*, vol. 35, no. 9, pp. 2069–2084, Sept. 2017.
- [10] J. Palacios, D. Donno, and J. Widmer, "Tracking mm-Wave channel dynamics: fast beam training strategies under mobility," in *Proc. IEEE INFOCOM'17*, Atlanta, GA, USA, May 2017, pp. 1–9.
- [11] G. Brown, O. Koymen, and M. Branda, "The promise of 5G mmWave - how do we make it mobile?" *Light Reading Webinar*, Jun. 2016.
- [12] R. E. Fischer, B. Tadic-Galeb, P. R. Yoder, and R. Galeb, *Optical system design*. New York: McGraw Hill, 2000.
- [13] Z. Ghassemlooy, W. Popoola, and S. Rajbhandari, *Optical wireless communications: system and channel modelling with Matlab*, CRC Press, 2012.
- [14] H. Burchardt, N. Serafimovski, D. Tsonev, S. Videv, and H. Haas, "VLC: Beyond point-to-point communication," *IEEE Commun. Mag.*, vol. 52, no. 7, pp. 98–105, Jul. 2014.
- [15] A. Papoulis and S. U. Pillai, *Probability, Random Variables, and Stochastic Processes*. Tata McGraw-Hill Education, 2002.
- [16] G. Li, S. Yang, Y. Chen, and Z. P. Nie, "A novel electronic beam steering technique in time modulated antenna array," *Progress In Electromagnetics Research*, vol. 97, pp. 391–405, 2009.
- [17] T. S. Rappaport, G. R. MacCartney, M. K. Samimi, and S. Sun, "Wide-band millimeter-wave propagation measurements and channel models for future wireless communication system design," *IEEE Trans. Commun.*, vol. 63, no. 9, pp. 3029–3056, Sept. 2015.
- [18] G. R. MacCartney Jr., M. K. Samimi, and T. S. Rappaport, "Exploiting directionality for millimeter-wave wireless system improvement," in *Proc. IEEE ICC'15*, London, UK, Jun. 2015, pp. 1–7.
- [19] X. Wu, C.-X. Wang, J. Sun, J. Huang, R. Feng, Y. Yang, and X. Ge, "60-GHz millimeter-wave channel measurements and modeling for indoor office environments," *IEEE Trans. Antennas Propag.*, vol. 65, no. 4, pp. 1912–1924, Apr. 2017.
- [20] Y. Tan, J. Huang, R. Feng, and C.-X. Wang, "A study of angular stationarity of 5G millimeter wave channels," in *Proc. ISWCS'17*, Bologna, Italy, Aug. 2017.